

Accepted Manuscript

Metal-organic framework-801 for efficient removal of fluoride from water

Xue-Hui Zhu, Cheng-Xiong Yang, Xiu-Ping Yan

PII: S1387-1811(17)30654-6

DOI: [10.1016/j.micromeso.2017.10.001](https://doi.org/10.1016/j.micromeso.2017.10.001)

Reference: MICMAT 8577

To appear in: *Microporous and Mesoporous Materials*

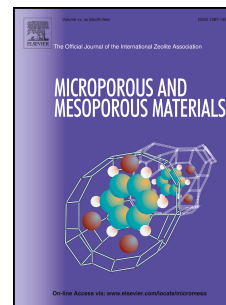
Received Date: 28 July 2017

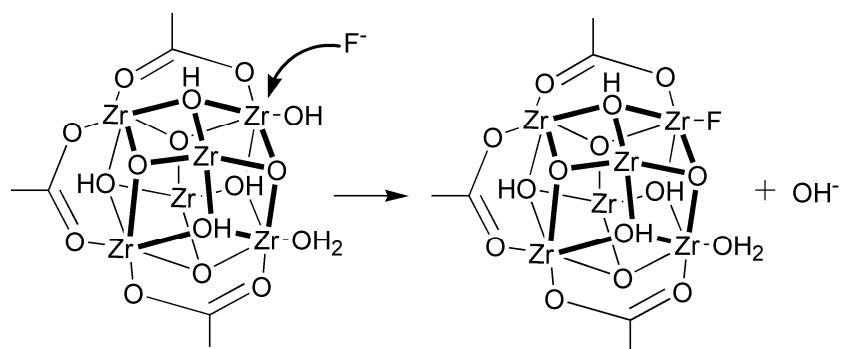
Revised Date: 8 September 2017

Accepted Date: 4 October 2017

Please cite this article as: X.-H. Zhu, C.-X. Yang, X.-P. Yan, Metal-organic framework-801 for efficient removal of fluoride from water, *Microporous and Mesoporous Materials* (2017), doi: 10.1016/j.micromeso.2017.10.001.

This is a PDF file of an unedited manuscript that has been accepted for publication. As a service to our customers we are providing this early version of the manuscript. The manuscript will undergo copyediting, typesetting, and review of the resulting proof before it is published in its final form. Please note that during the production process errors may be discovered which could affect the content, and all legal disclaimers that apply to the journal pertain.





Metal-organic framework-801 for efficient removal of fluoride from water

Xue-Hui Zhu^a, Cheng-Xiong Yang^{*,a}, Xiu-Ping Yan^{*,a,b,c}

^a *College of Chemistry, Research Center for Analytical Sciences, Tianjin Key Laboratory of Molecular Recognition and Biosensing, Nankai University, Tianjin 300071, China*

^b *State Key Laboratory of Food Science and Technology, Institute of Analytical Food Safety, School of Food Science and Technology, Jiangnan University, Wuxi 214122, China*

^c *Collaborative Innovation Center of Chemical Science and Engineering (Tianjin), Tianjin 300071, China*

*Corresponding Author

E-mail: xpyan@nankai.edu.cn

Phone: (86) 22-23506075

Fax: (86) 22-23506075

ABSTRACT

Fluoride excess in water is harmful to human beings. Adsorption is an effective way to remove fluoride in water. Exploring novel and efficient sorbents for fluoride adsorption is very necessary and challenging. In this work, the fluoride adsorption behavior of zirconium fumarate metal-organic framework-801 (MOF-801) in water is studied through batch adsorption experiments. MOF-801 has high and stable adsorption efficiency at pH 2-10. The fluoride adsorption capacity on MOF-801 is neither affected by high ion strength nor other anions including Cl^- , NO_3^- and SO_4^{2-} . The fluoride adsorption on MOF-801 follows a pseudo-second-order model and the Langmuir equation. The fluoride adsorption capacity of MOF-801 is 40 mg g^{-1} at 303 K, changing little with temperature. The effective defluoridation of MOF-801 resulted from the ion exchange of fluoride ions and hydroxyl group in MOF-801. The practical use of MOF-801 for fluoride adsorption from real water sample reveals the potential of MOF-801 as an efficient adsorbent for the removal of fluoride from water.

Keywords:

Defluoridation

Fluoride

Metal-Organic Frameworks

Adsorption

Water

1. Introduction

Drinking water safety is an important issue to human beings. High concentration of fluoride in drinking water can be very harmful. To protect human health from the disturbance of fluoride, the world health organization (WHO) recommends the guideline of fluoride in drinking water is 1.5 mg L^{-1} [1]. Both natural sources (dissolution of fluoride-rich rocks and soils in water) and anthropogenic sources (discharge of fluorine-containing industrial wastewater) can cause high concentration of fluoride in the water. Long-term consumption of water with fluoride concentration higher than 1.5 mg L^{-1} can cause chronic fluorosis such as dental fluorosis and skeletal fluorosis [2-4]. Therefore, reduction of the fluoride concentration in water is quite important for human beings.

Plenty of methods including precipitation-coagulation [5], membrane technology [6,7], ion-exchange [8] and adsorption [9,10] have been attempted in recent decades to reduce fluoride in water to meet the drinking water safety level. Among all of these methods, adsorption of fluoride on adsorbents receives increasing attention due to its advantages of easy design and operation, and low cost [2]. Different kinds of adsorbents such as metal-based adsorbents [11-13], carbon-based adsorbents [14,15], natural materials [16], and biosorbents [17-19] have been used to remove fluoride from water. Recently, zirconium-based materials have been proved to be good candidates in fluoride adsorption because of the high affinity of tetravalent metal ions Zr (IV) to the high electronegativity fluoride ion. Moreover, zirconium-based materials have good thermal and chemical stability [20-23].

Metal-organic frameworks (MOFs) are multifunctional porous materials potential in diverse areas [24]. Recently, MOFs have also been utilized as novel adsorbents for the

adsorption of fluoride because of high surface area, rich surface functional groups, and highly ordered atomic arrangement [25]. For example, MIL-53(Fe), MIL-53(Cr), ZIF-7, ZIF-8, UiO-66(Zr), CAU-6, MIL-96(Al), MIL-88A(Fe) and NH₂-UiO-66(Zr) have been successful applied for fluoride adsorption from water [26-30]. Among all of these MOFs, zirconium-based MOFs display higher adsorption capacity and good stability in the fluoride solution.

Zirconium fumarate framework MOF-801 (Zr₆O₄(OH)₄(fumarate)₆·xH₂O), constructed from ZrCl₄ and fumaric acid, has good water stability, large surface area, and UiO-66 type network topology [31-35], so MOF-801 is a good adsorbent for the removal of fluoride from water. Herein, we report the adsorption behavior and application of MOF-801 for efficient adsorption and removal of fluoride from water. MOF-801 offers fast kinetics and high capacity for the adsorption of fluoride at pH 2-10. The effect of adsorbent dose, ionic strength, pH and co-existing anions on the adsorption of fluoride are studied in detail. The adsorption mechanism of MOF-801 for fluoride is also discussed.

2. Materials and methods

2.1. Preparation of MOF-801

MOF-801 was synthesized according to Ren *et al.* with minor modification [35]. Typically, ZrCl₄ (0.2411 g), fumaric acid (0.3598 g) and formic acid (3.90 mL) and ultrapure water (20 mL) were mixed under ultrasonication, and then transferred into a 30-mL Teflon-lined stainless-steel autoclave. The autoclave was sealed and placed in oven at 120 °C for 24 h. After cooling to room temperature, the white powder was thoroughly washed with ultrapure water and absolute ethanol sequentially, then dried at 80 °C for 24 h.

2.2. Characterization

D/max-2500 X-ray diffractometer (Rigaku, Japan) and SS-550 scanning electron microscope (Shimadzu, Japan) were used to obtain the X-ray diffraction spectrometry (XRD) patterns and scanning electron microscopy (SEM) images, respectively. An ASAP 2020 automatic surface area and pore size analyzer (Micromeritics, USA) was used to measure the Brunauer-Emmett-Teller (BET) data of MOF-801 at 77 K using nitrogen. An ESCALAB 250Xi spectrometer (Thermo Fisher Scientific, USA) and SU-1510 scanning electron microscope (Hitachi, Japan) were used for X-ray photoelectron spectrometer (XPS) experiments and energy-dispersive X-ray spectroscopy (EDX) analysis, respectively. A Malvern Nano ZS90 Zetasizer (Malvern, UK) was used to measure the zeta potential of adsorbent, while a fluoride ion selective electrode PF-1-01 (Leici, China) was used to determine fluoride in aqueous solution.

2.3. Adsorption experiments

The effect of adsorbent dose on fluoride removal was tested by suspending different doses of MOF-801 in fluoride solution (20 mL, 10 mg L⁻¹) in a 50-mL plastic centrifuge tube. The mixture was shaken at 303K with a speed of 200 rpm for 2 h. The supernatant was then filtered with a 0.22- μ m cellulose membrane. The filtrate was collected and analyzed for the concentration of fluoride. Finally, the adsorption capacity of fluoride was calculated according to Eq. (1):

$$q_e = \frac{(C_0 - C_e)V}{m} \quad (1)$$

where C_0 and C_e refer to the initial and equilibrium concentration of fluoride (mg L⁻¹), respectively, V the volume of the fluoride solution (L), and m the amount of the MOF-801 (g).

The adsorption kinetics was studied at 303 K with 120 mL of fluoride solution (5 and 10 mg L⁻¹). Each 6 mL of mixture was taken out at a specified time (5-240 min) and filtered for fluoride determination.

The adsorption isotherms were conducted in the concentration range of 10-120 mg L⁻¹ fluoride at 293-323 K. The effect of co-existing anions Cl⁻, NO₃⁻, SO₄²⁻, HCO₃⁻, PO₄³⁻ of 10, 50 and 100 mg L⁻¹ was also investigated. Fluoride solutions with different ionic strengths were prepared with sodium chloride.

The effect of pH was studied at pH 2-13. The pH value of the fluoride solution (10 mg L⁻¹) was adjusted with 0.1 M NaOH or 0.1 M HCl. The MOF-801 was then added for adsorption. The fluoride solution after adsorption was adjusted with total ionic strength adjustment buffer (TISAB) solution (pH=5.0-5.5). The fluoride solution after adjusting with TISAB was then measured using a fluoride ion selective electrode.

3. Results and discussion

3.1. Characterization of MOF-801

The as-synthesized MOF-801 was characterized by XRD, N₂ adsorption, SEM and TGA experiments (Fig. 1 and Fig. S3). The XRD pattern of the as-synthesized MOF-801 is in accordance with the simulated pattern, suggesting the successful synthesis of MOF-801 (Fig. 1a). No significant change in the XRD pattern of MOF-801 after fluoride adsorption indicates the good stability of MOF-801 in fluoride solution. The N₂ adsorption-desorption data reveal the surface area, pore diameter and pore volume of as-synthesized MOF-801 are 725 m² g⁻¹, 0.55 Å and a 0.40 cm³ g⁻¹, respectively (Fig. 1b), which are all similar to the data in the reported literatures [31,34,35].

The SEM image shows the as-synthesized MOF-801 has uniform octahedron shaped morphology with the particle size of ca. 400 nm (Fig. 1c). The morphology of MOF-801 did not change after fluoride adsorption (Fig. 1d), proving the good stability of MOF-801 in the adsorption process. The TGA curve reveals the MOF-801 is stable up to 350 °C (Fig. S3). The weight loss before 100 °C was attributed to the loss of absorbed water in MOF-801 [32].

Fig. 1. Here

3.2. Effect of adsorbent dose

The effect of MOF-801 dose on fluoride removal was first studied with 10 mg L⁻¹ of fluoride solution at 303 K (Fig. 2a). The fluoride removal efficiency increased as the adsorbent dose increased from 0.2 to 0.7 g L⁻¹, then leveled off as the adsorbent dose further increased from 0.7 to 1.1 g L⁻¹. Therefore, 0.7 g L⁻¹ was selected to ensure the fluoride removal in the following experiments.

Fig. 2. Here

3.3. Effect of pH on fluoride removal

The pH of natural water often varies with its geographic location, weather and environment. In addition, the fluoride species was also dependent on the solution pH value. Therefore, the effect of pH on fluoride removal was examined with 10 mg L⁻¹ of fluoride solution at 303 K (Fig. 2b). MOF-801 gave high and stable removal efficiency from pH 2 to pH 10. It is worth mentioning that even at pH 10, the equilibrium concentration of fluoride after adsorption (0.97 mg L⁻¹) was smaller than the WHO guideline of fluoride in drinking water (1.5 mg L⁻¹), showing the good performance of MOF-801 for adsorption and removal of fluoride from water. The pH values of fluoride solution used in this work were all in the range of 2-10. So,

no pH adjusting was needed for the following experiments. Further increase of the pH led to a significant decrease of the fluoride removal efficiency. To confirm whether such decline of the fluoride removal efficiency at higher pH (>10) was caused by the electrostatic interaction between the fluoride and MOF-801, the pH dependence of the Zeta potential of MOF-801 was evaluated (Fig. 2b). The MOF-801 was negatively charged at pH > 7, suggesting electrostatic repulsion could happen between negatively charged MOF-801 and fluoride at pH 8-11. In addition, the Zeta potentials of MOF-801 at pH 10 (-44.1 mV) and 11 (-44.4 mV) were almost the same. However, the fluoride removal efficiency on MOF-801 at pH 10 and 11 decreased from 90% to 61%, revealing the electrostatic repulsion cannot fully explain the decline of fluoride removal efficiency at high pH. The possible reason is the competition of higher concentration of OH⁻ at pH 11 with fluoride for the active sites on MOF-801 [28].

Fig. 3. Here

Table 1 Here

3.4. Effect of contact time

The effect of contact time on fluoride removal was tested with 5 and 10 mg L⁻¹ of fluoride solutions (Fig. 3a). The adsorption of fluoride reached equilibrium within 10 min for 5 mg L⁻¹ of fluoride solution, showing the fast adsorption kinetics of MOF-801 for fluoride. 97% of fluoride was removed within 40 min for 10 mg L⁻¹ of fluoride solution although the adsorption equilibrium was reached within 2 h. The equilibrium adsorption capacity of MOF-801 for fluoride at the initial concentration of 5 and 10 mg L⁻¹ are 7.1 and 13.6 mg g⁻¹, respectively. The results suggest higher initial concentration is favorable for the adsorption of fluoride on MOF-801.

The pseudo-first-order and pseudo-second-order kinetic models were applied to study the fluoride adsorption kinetics on MOF-801. The linear forms of pseudo-first-order rate and pseudo-second-order rate are expressed as Eqs. (2) and (3), respectively [27,28]:

$$\ln(q_e - q_t) = \ln q_e - \frac{k_1}{2.303} t \quad (2)$$

$$\frac{t}{q_t} = \frac{1}{k_2 q_e^2} + \frac{1}{q_e} t \quad (3)$$

where q_e and q_t are the amounts of fluoride adsorbed on MOF-801 (mg g^{-1}) at equilibrium and at time t (min), respectively. k_1 and k_2 are the rate constants of pseudo-first-order kinetics and pseudo-second-order kinetics, respectively.

Fig. S1a and Fig. 3b show the fitted lines of pseudo-first-order and pseudo-second-order models, respectively. The corresponding kinetic constants and determination coefficients (R^2) data are summarized in Table 1. The determination coefficients (R_1^2) of pseudo-first-order model for 5 and 10 mg L^{-1} of fluoride solutions are 0.381 and 0.841, respectively, revealing the fluoride adsorption process cannot be explained by pseudo-first-order kinetic model. In contrast, the determination coefficients (R_2^2) of pseudo-second-order model are both larger than 0.999 for 5 and 10 mg L^{-1} of fluoride solution. At the same time, the calculated adsorption capacities using pseudo-second-order equation were similar to those obtained from experiments. Therefore, the fluoride adsorption kinetics on MOF-801 followed the pseudo-second-order kinetics.

Table 2 Here

3.5. Adsorption isotherms

To further study the adsorption behavior and to obtain the maximum fluoride adsorption capacity of MOF-801, fluoride adsorption isotherms were investigated with 10-120 mg L⁻¹ of fluoride solutions at 293-323 K (Fig. 3c). The adsorption capacity increased steadily with the equilibrium fluoride concentration from 0 to 60 mg L⁻¹, showing favorable adsorption of fluoride on MOF-801 at higher initial concentration. No obvious change of the adsorption capacity in the equilibrium fluoride concentration from 60 to 100 mg L⁻¹ suggests the achievement of adsorption saturation of fluoride on MOF-801. The adsorption isotherms at 293, 303, 313 and 323 K almost overlapped with each other, indicating no significant effect of temperature on the fluoride adsorption capacities of MOF-801 in the range of 293-323 K. The results show that MOF-801 had good and stable fluoride adsorption capacity at most natural water temperatures.

Langmuir (Eq. (4)) and Freundlich equations (Eq. (5)) [27] were used to evaluate the adsorption data of MOF-801:

$$\frac{C_e}{q_e} = \frac{1}{q_m K_L} + \frac{1}{q_m} C_e \quad (4)$$

$$\ln q_e = \ln K_F + \frac{1}{n} \ln C_e \quad (5)$$

where C_e is equilibrium concentration (mg L⁻¹), q_e is the adsorption capacity at equilibrium (mg g⁻¹), q_m is the maximum adsorption capacity (mg g⁻¹) for Langmuir isotherms at a specific temperature, and K_L is the Langmuir constant which indicates the affinity of fluoride towards the adsorbent. K_F and n are Freundlich constants relating to adsorption capacity and adsorption intensity, respectively.

Table 3 Here

The fitting curves for Langmuir equation and the Freundlich equation are illustrated in Fig. 3d and Fig. S1b, respectively. The calculated parameters from the fitting curves are summarized in Table 2. The data show that Langmuir equation is better than Freundlich equation to describe the adsorption process of fluoride on MOF-801. The Langmuir model assumes that the adsorbent has homogeneous surface active sites while adsorbate is monolayer adsorbed on the adsorbent [17,27]. The monolayer adsorption suggests the adsorption of fluoride on MOF-801 was chemisorption. In the meantime, the dimensionless constant separation factor R_L of Langmuir isotherm at 303 K can be used to further explain the favorability of fluoride adsorption on MOF-801 (Table 3). R_L is defined as Eq. (6):

$$R_L = \frac{1}{1 + K_L C_0} \quad (6)$$

where C_0 is the initial fluoride concentration, K_L is the Langmuir isotherm constant. R_L is the dimensionless constant separation factor of Langmuir isotherm, where $R_L < 1$ represents the favorable adsorption and $R_L > 1$ represents the unfavorable adsorption processes [36]. The R_L values of MOF-801 in the initial fluoride concentration range of 10-120 mg L⁻¹ are less than 1 (Table 3), revealing the favorable adsorption of fluoride on MOF-801 [17,36]. In addition, the negative Gibbs free energy change ($\Delta G < 0$) further suggests the spontaneous adsorption of fluoride on MOF-801 (Table S1 and Fig. S2).

3.6. Effect of co-existing anions

Effect of co-existing anions including Cl⁻, NO₃⁻, SO₄²⁻, HCO₃⁻ and PO₄³⁻ in the range of 10-100 mg L⁻¹ on fluoride removal efficiency of MOF-801 was studied with 10 mg L⁻¹ of fluoride solution (Fig. 4a). The Cl⁻, NO₃⁻ and SO₄²⁻ have little effect on fluoride removal efficiency even though

their concentrations (100 mg L^{-1}) are ten times higher than that of fluoride. However, increase of the co-existing concentration of HCO_3^- and PO_4^{3-} from 0 to 100 mg L^{-1} led to the decrease of removal efficiency from 98% to 77% and 34%, respectively, likely due to the electrostatic repulsion, high pH values of HCO_3^- and PO_4^{3-} solution and the competition of HCO_3^- and PO_4^{3-} with fluoride for adsorption. The pH values for NaHCO_3 (8.6) and Na_3PO_4 (10.9) solutions at 100 mg L^{-1} , together with the electrostatic repulsion between the negatively charged MOF-801 and F^- under these pH values gave negative effect on fluoride removal efficiency (Fig. 2b). However, the fluoride removal efficiency was reduced to 61% at pH 11 (Fig. 2b). While for Na_3PO_4 solution (pH = 10.9), the fluoride removal efficiency was reduced to 34% (Fig. 4a), suggesting the high pH value and the electrostatic repulsion are not the whole reason for the decrease of fluoride removal efficiency. In addition, HCO_3^- and PO_4^{3-} interfere with the fluoride adsorption through competition of fluoride active adsorption sites on MOF-801. The $[\text{HCO}_3^-]/[\text{CO}_3^{2-}]$ is 97.8% at pH 8.6, so HCO_3^- is the main speciation absorbed. The above results indicate that the electrostatic repulsion, the high pH value and the competitive adsorption of PO_4^{3-} and HCO_3^- together lead to the decrease of fluoride adsorption efficiency.

Fig. 4. Here

3.7. Effect of ionic strength

Effect of ionic strength [37] on fluoride adsorption capacity was evaluated in an ionic strength range of 0.018-0.361 M (Fig. 4b). The results reveal that ionic strength had little effect on fluoride adsorption capacity, which is quite favorable for the practical application of MOF-801 for fluoride removal in real water sample with high ionic strength.

3.8. Adsorption mechanism

The FT-IR spectra of MOF-801 before and after fluoride adsorption ($C_0(\text{F}^-) = 10 \text{ mg L}^{-1}$) were studied to elucidate the adsorption mechanism (Fig. 5a). The peak at 3397 cm^{-1} of MOF-801 before adsorption can be ascribed to the stretching vibration of hydroxyl group. The peaks at 1578 and 1405 cm^{-1} are the characteristic peaks of asymmetric and symmetric stretching vibration of carboxylate group for MOF-801 before adsorption [33]. No changes were observed for all the peaks of carboxylate group on MOF-801 after fluoride adsorption (Fig. 5a). However, the characteristic peak of hydroxyl group on MOF-801 shifted from 3397 cm^{-1} to 3404 cm^{-1} after fluoride adsorption, suggesting the hydroxyl group on MOF-801 may be the active site that plays significant roles in fluoride adsorption [25,26].

The EDX spectra of MOF-801 before and after fluoride adsorption ($C_0(\text{F}^-) = 10 \text{ mg L}^{-1}$) were further studied (Fig. 5c and 5d). The appearance of the new peak for fluoride after adsorption indicates the successfully adsorption of fluoride on MOF-801 [23]. In addition, the increase of the F content (from 0 to 1.9%) as well as the decrease of the O content (from 41.0 to 38.7%) after adsorption suggests the fluoride may compete or replace the hydroxyl group on MOF-801 during the adsorption process.

Fig. 5. Here

The effect of MOF-801 addition on the pH of water and fluoride solutions (10 and 100 mg L^{-1}) was investigated in the initial solution pH range of 3-11. The plots of the final solution pH at equilibrium in the presence of MOF-801 against the initial solution pH in the absence of MOF-801 are shown in Fig. 5b. MOF-801 has strong buffering effect in the initial pH range of 3-11 due to the interaction of MOF-801 with the H^+ and OH^- in the aqueous solution. Such buffering effect on the solution pH was also observed on other porous materials [38]. The final pH of the

solution was near 4.0, 5.0 and 7.0 in water, 10 and 100 mg L⁻¹ fluoride solution in the initial pH range of 5-10, respectively. The final pH of MOF-801 in water is much lower than that of fluoride solution with the same initial pH values (Fig. 5b), suggesting that the adsorption of fluoride on MOF-801 led to the increase of the pH due to the release of OH⁻ from MOF-801 into solution via fluoride anion exchange. The final pH values of 10 and 100 mg L⁻¹ fluoride solution are slightly higher than that of water when the initial pH value was 3. The higher fluoride adsorption capacities of MOF-801 in 10 and 100 mg L⁻¹ fluoride solution may lead to the release of more OH⁻ than in water based on the anion exchange mechanism. However, pH 3 offers higher H⁺ concentration and more powerful to neutralize the released OH⁻ than other pH values greater than 3.

Fig. 6. Here

Table 4 Here

The ion exchange between F⁻ and OH⁻ on MOF-801 was further proved by XPS experiments (Fig. 6 and Table 4). The appearance of F1s peak in wide scan spectra of MOF-801 after fluoride adsorption reveals the adsorption of fluoride on the MOF-801 (Fig. 6a) [23]. Changing the initial fluoride solution from 10 to 100 mg L⁻¹ led to the increase of F1s peak intensity, further indicating higher initial fluoride concentration was beneficial for fluoride adsorption on MOF-801 (Fig. 6b). The peak of Zr3d_{5/2} shifted from 182.63 eV to 182.67 and 182.77 eV after adsorption of fluoride at 10 and 100 mg L⁻¹, respectively (Fig. 6c), indicating that the interaction between the zirconium in MOF-801 and fluoride is responsible for the adsorption of fluoride on MOF-801 [17,23,39]. O1s spectra of MOF-801 can be divided into three peaks, zirconium oxide bond (Zr-O, at about 530.2 eV), zirconium hydroxyl bond (Zr-OH, at about 531.7 eV) and water

(H₂O, at about 532.8 eV) [21,38,40]. Specific binding energies of these peaks and their percentages are listed in Table 4. The Zr-OH percentages of MOF-801 decreased after fluoride adsorption. Increase of the initial fluoride concentration from 10 to 100 mg L⁻¹ gave significant decrease of the Zr-OH percentage from 60.93% to 56.13% along with the increase of fluoride adsorption capacity from 13.6 to 38.6 mg g⁻¹ at 303 K, suggesting the ion exchange of Zr-OH with F⁻ during adsorption.

Table 5 Here

3.9. Adsorption of fluoride from real water sample

The MOF-801 was applied to treat the real surface water sample collected from Tanggu District, Tianjin, China. Table 5 shows the pH and the concentration of F⁻, HCO₃⁻, Cl⁻ and SO₄²⁻ in the water sample before and after adsorption. Ion chromatography results show no detected PO₄³⁻ in the studied real water sample (Fig. S4). The F⁻ concentration in the water sample was 4.54 mg L⁻¹, which was much higher than the WHO guideline of 1.5 mg L⁻¹. The concentration of HCO₃⁻, Cl⁻, and SO₄²⁻ were also much higher than 100 mg L⁻¹, which means the complex nature and high ionic strength of the real water sample. After adsorption with MOF-801 at a 0.7 g L⁻¹ dose, the fluoride concentration was greatly reduced to 2.0 mg L⁻¹, which was close to the WHO guideline of 1.5 mg L⁻¹. The decrease of the adsorption capacity of MOF-801 in the real water sample (3.6 mg g⁻¹ compared to 7.1 mg g⁻¹ in standard fluoride aqueous solution) resulted from the serious disturbance of the high concentration HCO₃⁻ (460 mg L⁻¹) in the real water sample (Table 5 and Fig. 4a). The decrease of HCO₃⁻ concentration after adsorption (from 460 to 300 mg L⁻¹) reveals that the HCO₃⁻ was also adsorbed on MOF-801 to compete with fluoride for the

adsorption sites on MOF-801. The Cl^- and SO_4^{2-} could not be adsorbed on MOF-801 due to their unchanged concentration before and after adsorption (Table 5). Increasing the MOF-801 dose to 1.0 g L^{-1} reduced the fluoride concentration in the water sample below the WHO guideline of 1.5 mg L^{-1} (Fig. 7), showing the relatively good adsorption performance of MOF-801 for fluoride from complex real water samples. The UiO-66(Zr) was further synthesized (Fig. S5) and studied for comparison. MOF-801 gave better performance to remove fluoride from real water sample than UiO-66(Zr) (Table 5).

Fig. 7. Here

4. Conclusion

We have reported the application of MOF-801 as an efficient adsorbent for fluoride removal with fast adsorption kinetics and large adsorption capacity. MOF-801 gives good performance for fluoride removal in a wide pH range of 2-10, high ionic strength and good anti-interference capability for the co-existing ions. MOF-801 also shows higher adsorption capacity (40 mg g^{-1}) than lots of reported adsorbents [28]. The stable adsorption capacity of MOF-801 for fluoride in a temperature range of 293-323 K also makes it convenient for practical use. The results reveal that the ion exchange of fluoride ions and hydroxyl group in MOF-801 plays significant roles for efficient fluoride removal in water. The practical use of MOF-801 for fluoride adsorption from real water sample reveals the potential of MOF-801 as novel adsorbent for fluoride adsorption from water.

Acknowledgment

This work was supported by the National Basic Research Program of China (2015CB932001) the Fundamental Research Funds for Central Universities (JUSRP51714B), and Open Funds of the State Key Laboratory of Electroanalytical Chemistry (SKLEAC201705).

References

- [1] S. Jagtap, M.K. Yenkie, N. Labhsetwar, S. Rayalu, *Chem. Rev.* 112 (2012) 2454-2466.
- [2] A. Bhatnagar, E. Kumar, M. Sillanpää, *Chem. Eng. J.* 171 (2011) 811-840.
- [3] M. Mohapatra, S. Anand, B.K. Mishra, D.E. Giles, P. Singh, *J. Environ. Manage.* 91 (2009) 67-77.
- [4] L.H. Velazquez-Jimenez, E. Vences-Alvarez, J.L. Flores-Arciniega, H. Flores-Zuñiga, J.R. Rangel-Mendez, *Sep. Purif. Technol.* 150 (2015) 292-307.
- [5] W.X. Gong, J.H. Qu, R.P. Liu, H.C. Lan, *Colloid Surface A.* 395 (2012) 88-93.
- [6] A. Tor, *J. Hazard. Mater.* 141 (2007) 814-818.
- [7] J.Y. He, K. Chen, X.G. Cai, Y.L. Li, C.M. Wang, K.S. Zhang, Z. Jin, F.L. Meng, X.G. Wang, L.T. Kong, J.H. Liu, *J. Colloid Interface Sci.* 490 (2017) 97-107.
- [8] N. Viswanathan, S. Meenakshi, *J. Hazard. Mater.* 162 (2009) 920-930.
- [9] X.P. Liao, B. Shi, *Environ. Sci. Technol.* 39 (2005) 4628-4632.
- [10] L.H. Velazquez-Jimenez, R.H. Hurt, J. Matos, J.R. Rangel-Mendez, *Environ. Sci. Technol.* 48 (2014) 1166-1174.
- [11] B. Zhao, Y. Zhang, X.M. Dou, X.M. Wu, M. Yang, *Chem. Eng. J.* 185-186 (2012) 211-218.
- [12] C.Y. Jing, J.L. Cui, Y.Y. Huang, A. Li, *ACS Appl. Mater. Interfaces* 4 (2012) 714-720.

- [13] Z. Jin, Y. Jia, K.S. Zhang, L.T. Kong, B. Sun, W. Shen, F.L. Meng, J.H. Liu, *J. Alloy. Compd.* 675 (2016) 292-300.
- [14] E. Vences-Alvarez, L.H. Velazquez-Jimenez, L.F. Chazaro-Ruiz, P.E. Diaz-Flores, J.R. Rangel-Mendez, *J. Colloid Interface Sci.* 455 (2015) 194-202.
- [15] M.H. Dehghani, G.A. Haghghat, K. Yetilmezsoy, G. McKay, B. Heibati, I. Tyagi, S. Agarwal, V.K. Gupta, *J. Mol. Liq.* 216 (2016) 401-410.
- [16] Y. Çengelöğlü, E. Kir, M. Ersöz, *Sep. Purif. Technol.* 28 (2002) 81-86.
- [17] H.M. Cai, L.Y. Xu, G.J. Chen, C.Y. Peng, F. Ke, Z.Q. Liu, D.X. Li, Z.Z. Zhang, X.C. Wan, *Appl. Surf. Sci.* 375 (2016) 74-84.
- [18] L.Y. Xu, G.J. Chen, C.Y. Peng, H.H. Qiao, F. Ke, R.Y. Hou, D.X. Li, H.M. Cai, X.C. Wan, *Carbohydr. Polym.* 160 (2017) 82-89.
- [19] H. Paudyal, B. Pangenji, K.N. Ghimire, K. Inoue, K. Ohto, H. Kawakita, S. Alam, *Chem. Eng. J.* 195-196 (2012) 289-296.
- [20] C.F. Chang, C.Y. Chang, T.L. Hsu, *Desalination* 279 (2011) 375-382.
- [21] J. Wang, W.H. Xu, L. Chen, Y. Jia, L. Wang, X.J. Huang, J.H. Liu, *Chem. Eng. J.* 231 (2013) 198-205.
- [22] P.H. Chen, W.B. Zhang, M.L. Li, P. Ai, L. Tian, H.L. Jiang, *RSC Adv.* 6 (2016) 35859-35867.
- [23] S. Mohan, V. Kumar, D.K. Singh, S.H. Hasan, *RSC Adv.* 6 (2016) 87523-87538.
- [24] Z.Y. Gu, C.X. Yang, N. Chang, X.P. Yan, *Acc. Chem. Res.* 45 (2012) 734-745.
- [25] P. Kumar, A. Pournara, K.H. Kim, V. Bansal, S. Rapti, M.J. Manos, *Prog. Mater. Sci.* 86 (2017) 25-74.

- [26] X.D. Zhao, D.H. Liu, H.L. Huang, W.J. Zhang, Q.Y. Yang, C.L. Zhong, *Micropor. Mesopor. Mat.* 185 (2014) 72-78.
- [27] K.Y.A. Lin, Y.T. Liu, S.Y. Chen, *J. Colloid Interface Sci.* 461 (2016) 79-87.
- [28] N.T. Zhang, X. Yang, X.Y. Yu, Y. Jia, J. Wang, L.T. Kong, Z. Jin, B. Sun, T. Luo, J.H. Liu, *Chem. Eng. J.* 252 (2014) 220-229.
- [29] S. karmakar, J. Dechnik, C. Janiak, S. De, *J. Hazard. Mater.* 303 (2016) 10-20.
- [30] F. Ke, G. Luo, P.R. Chen, J. Jiang, Q.Y. Yuan, H.M. Cai, C.Y. Peng, X.C. Wan, *J. Porous Mater.* 23 (2016) 1065-1073.
- [31] G. Wißmann, A. Schaate, S. Lilienthal, I. Bremer, A.M. Schneider, P. Behrens, *Micropor. Mesopor. Mat.* 152 (2012) 64-70.
- [32] H. Furukawa, F. Gándara, Y.B. Zhang, J.C. Jiang, W.L. Queen, M.R. Hudson, O.M. Yaghi, *J. Am. Chem. Soc.* 136 (2014) 4369-4381.
- [33] M. Ganesh, P. Hemalatha, M.M. Peng, W.S. Cha, H.T. Jang, *Aerosol Air Qual. Res.* 14 (2014) 1605-1612.
- [34] G. Zahn, H.A. Schulze, J. Lippke, S. König, U. Sazama, M. Fröba, P. Behrens, *Micropor. Mesopor. Mat.* 203 (2015) 186-194.
- [35] J.W. Ren, N.M. Musyoka, H.W. Langmi, B.C. North, M. Mathe, X.D. Kang, S.J. Liao, *Int. J. Hydrogen Energ.* 40 (2015) 10542-10546.
- [36] S.K. Swain, S. Mishra, P. Sharma, T. Patnaik, V.K. Singh, U. Jha, R.K. Patel, R. K. Dey, *Ind. Eng. Chem. Res.* 49 (2010) 9846-9856.
- [37] N.A. Oladoja, B. Helmreich, H.A. Bello, *Chem. Eng. J.* 301 (2016) 166-177.
- [38] C. Zhang, Y.Z. Li, T.J. Wang, Y.P. Jiang, H.F. Wang, *Appl. Surf. Sci.* 363 (2016) 507-515.

[39] X.M. Dou, D. Mohan, C.U. Pittman Jr., S. Yang, Chem. Eng. J. 198-199 (2012) 236-245.

[40] D.D. Tang, G.K. Zhang, Chem. Eng. J. 283 (2016) 721-729.

ACCEPTED MANUSCRIPT

Figure Captions

Fig. 1. (a) XRD patterns of simulated MOF-801, as-synthesized MOF-801 before and after fluoride adsorption; (b) N₂ adsorption-desorption isotherms of MOF-801 (Inset: pore size distribution of MOF-801); (c) SEM images of as-synthesized MOF-801; (d) SEM images of MOF-801 after fluoride adsorption with the initial concentration of 10 mg L⁻¹ fluoride at 303 K.

Fig. 2. (a) Effect of MOF-801 dose on fluoride removal; (b) effect of pH on fluoride removal and the zeta potential of MOF-801 (T = 303 K, C₀ (F⁻) = 10 mg L⁻¹).

Fig. 3. (a) Effect of contact time on the fluoride removal efficiency of MOF-801 (T = 303 K, C₀ (F⁻) = 5 and 10 mg L⁻¹) (Inset, the enlarged fluoride removal efficiency before 15 min); (b) pseudo-second-order kinetics for the adsorption of fluoride on MOF-801 (T = 303 K, C₀ (F⁻) = 5 and 10 mg L⁻¹); (c) adsorption isotherms of MOF-801 (Inset, the enlarged adsorption isotherms at q_e less than 0.4 mg L⁻¹); (d) Langmuir fitting curves for the adsorption isotherms on MOF-801.

Fig. 4. (a) Effect of co-existing anions on fluoride removal efficiency of MOF-801 (T = 303 K; C₀ (F⁻) = 10 mg L⁻¹); (b) effect of ionic strength on fluoride adsorption capacity of MOF-801 (T = 298K, C₀ (F⁻) = 10 mg L⁻¹).

Fig. 5. (a) FT-IR spectra of MOF-801 before and after adsorption of 10 mg L⁻¹ fluoride solution; (b) changes in solution pH after adding MOF-801 (0.7 g L⁻¹) and fluoride adsorption (C₀ (F⁻) = 0, 10, 100 mg L⁻¹); EDX spectra of MOF-801 (c) before and (d) after fluoride adsorption (C₀ (F⁻) = 10 mg L⁻¹).

Fig. 6. XPS spectra of MOF-801 after adsorption of fluoride: (a) XPS wide scan spectrum, (b) F1s spectra, (c) Zr3d spectra (C₀ (F⁻) = 0, 10 and 100 mg L⁻¹); O1s spectra of MOF-801 after adsorption of fluoride at different concentrations (mg L⁻¹): (d) 0, (e) 10, (f) 100.

Fig. 7. Equilibrium fluoride concentration in real water sample with different MOF-801 dose.

ACCEPTED MANUSCRIPT

Table 1 Kinetic parameters for fluoride adsorption on MOF-801 at 303 K

C_0 (mg L ⁻¹)	$q_{e,exp}$ (mg g ⁻¹)	pseudo-first-order			pseudo-second-order		
		k_1 (min ⁻¹)	$q_{e,fitted}$ (mg g ⁻¹)	R^2	k_2 (min ⁻¹)	$q_{e,fitted}$ (mg g ⁻¹)	R^2
5	7.10	0.039	0.11	0.381	0.551	7.10	0.999
10	13.59	0.056	1.95	0.841	0.036	13.70	0.999

Table 2 Langmuir and Freundlich isotherm parameters for fluoride adsorption on MOF-801

Temp. (K)	Langmuir			Freundlich		
	q_{\max} (mg g ⁻¹)	K_L (L mg ⁻¹)	R^2	K_F (mg g ⁻¹) (L mg ⁻¹) ^{1/n}	n	R^2
293	38.20	0.493	0.997	21.35	7.42	0.959
303	40.26	0.400	0.995	19.98	6.16	0.983
313	39.94	0.370	0.995	18.97	5.75	0.992
323	38.83	0.336	0.995	17.84	5.58	0.980

Table 3 Calculated R_L values of MOF-801 based on the Langmuir model at 303 K

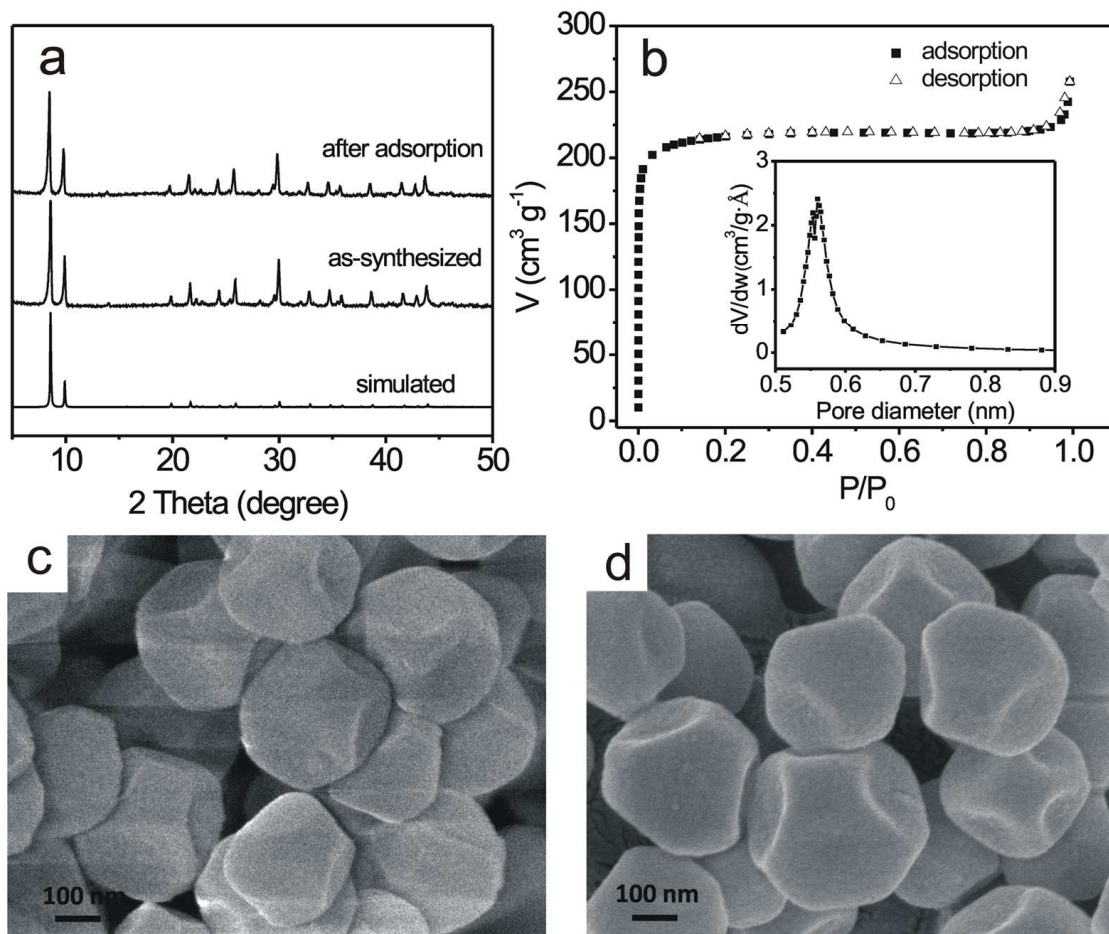
C_0 (mg L ⁻¹)	10	20	30	50	70	100	120
R_L	0.202	0.112	0.078	0.048	0.035	0.025	0.021

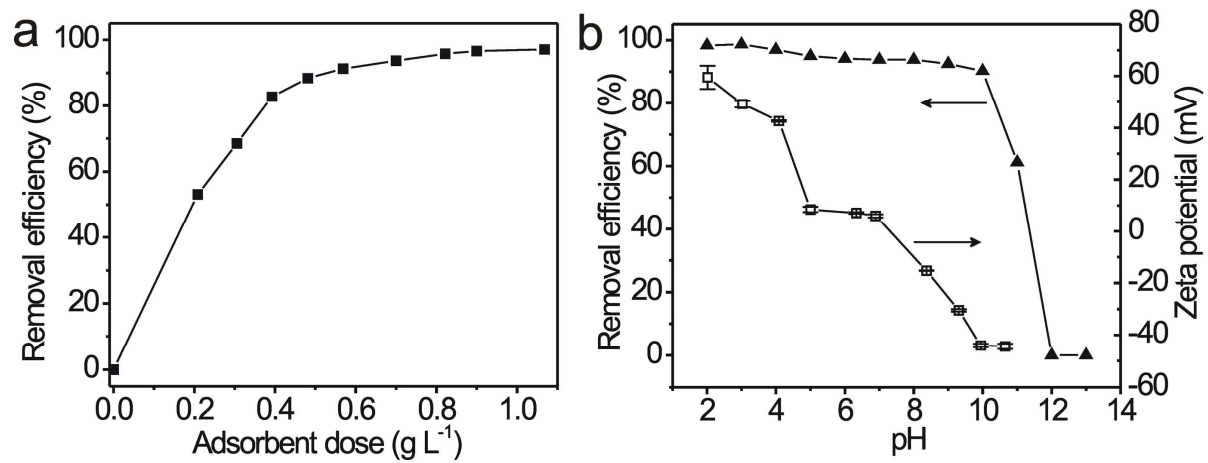
Table 4 O1s peak parameters of MOF-801 before and after fluoride adsorption

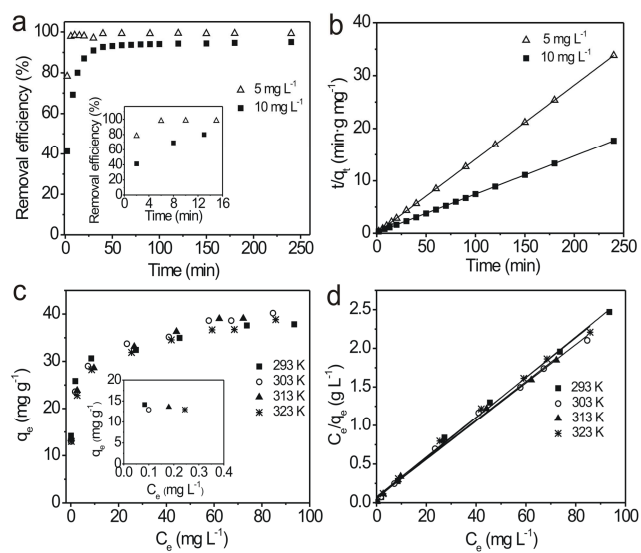
C_0 (F) (mg L ⁻¹)	Peak	B.E. (eV)	Percent (%)
0	Zr-O	530.18	26.8
	Zr-OH	531.72	65.4
	H ₂ O	532.85	7.9
10	Zr-O	530.18	29.3
	Zr-OH	531.72	60.9
	H ₂ O	532.85	9.8
100	Zr-O	530.20	33.9
	Zr-OH	531.70	56.1
	H ₂ O	532.85	10.0

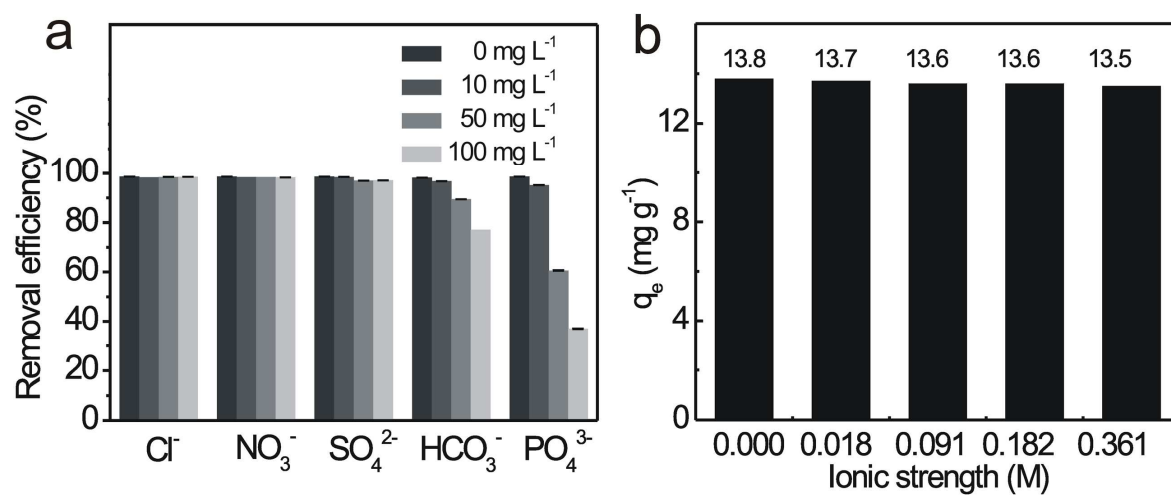
Table 5 Chemical parameters of a real surface water sample before and after adsorption of F⁻ on MOF-801 and UiO-66(Zr)

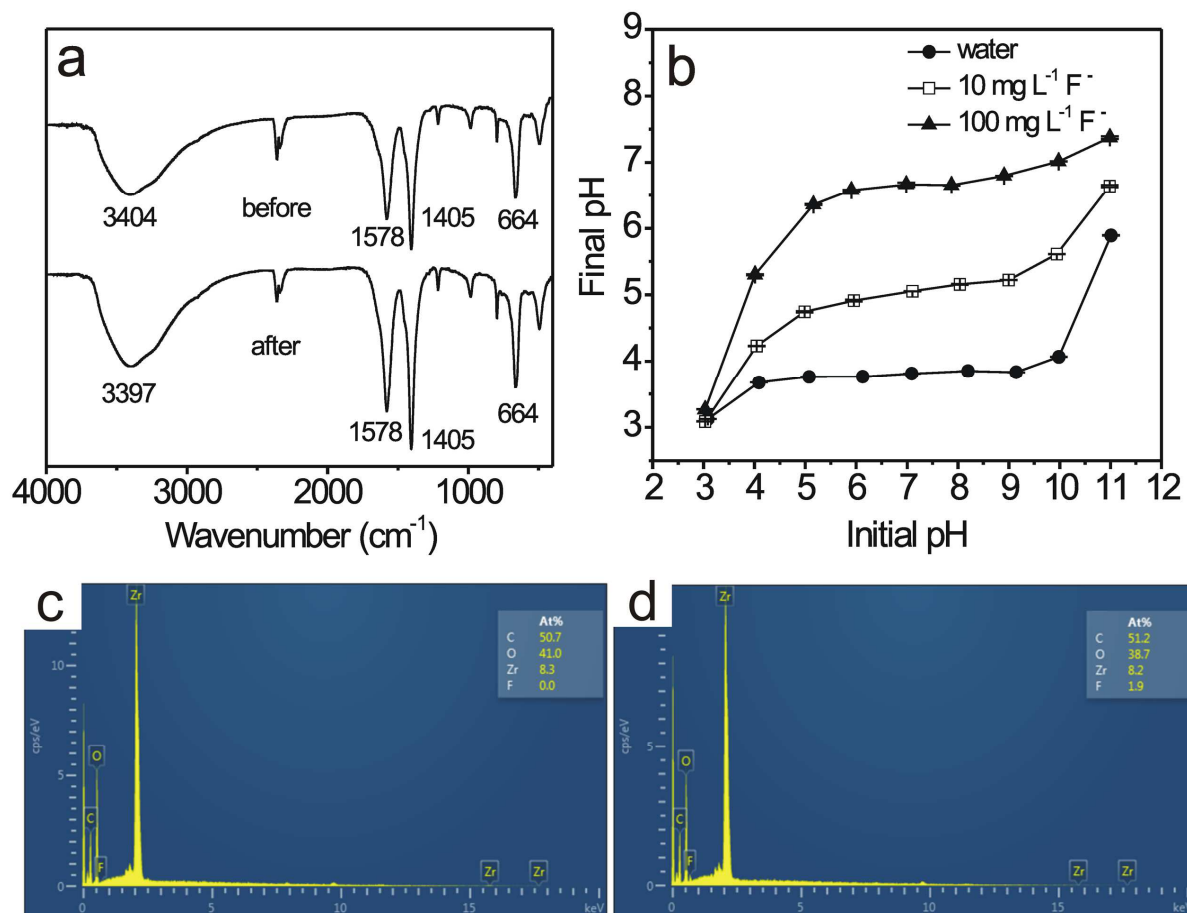
	Before adsorption	After adsorption	
		MOF-801	UiO-66(Zr)
pH	8.43 ± 0.02	7.35 ± 0.04	7.34 ± 0.01
C (F ⁻) (mg L ⁻¹)	4.54 ± 0.06	2.02 ± 0.01	2.60 ± 0.01
C (HCO ₃ ⁻) (mg L ⁻¹)	460 ± 2	299 ± 11	326 ± 3
C (Cl ⁻) (mg L ⁻¹)	750 ± 4	721 ± 2	715 ± 4
C (SO ₄ ²⁻) (mg L ⁻¹)	208 ± 2	202 ± 3	206 ± 1

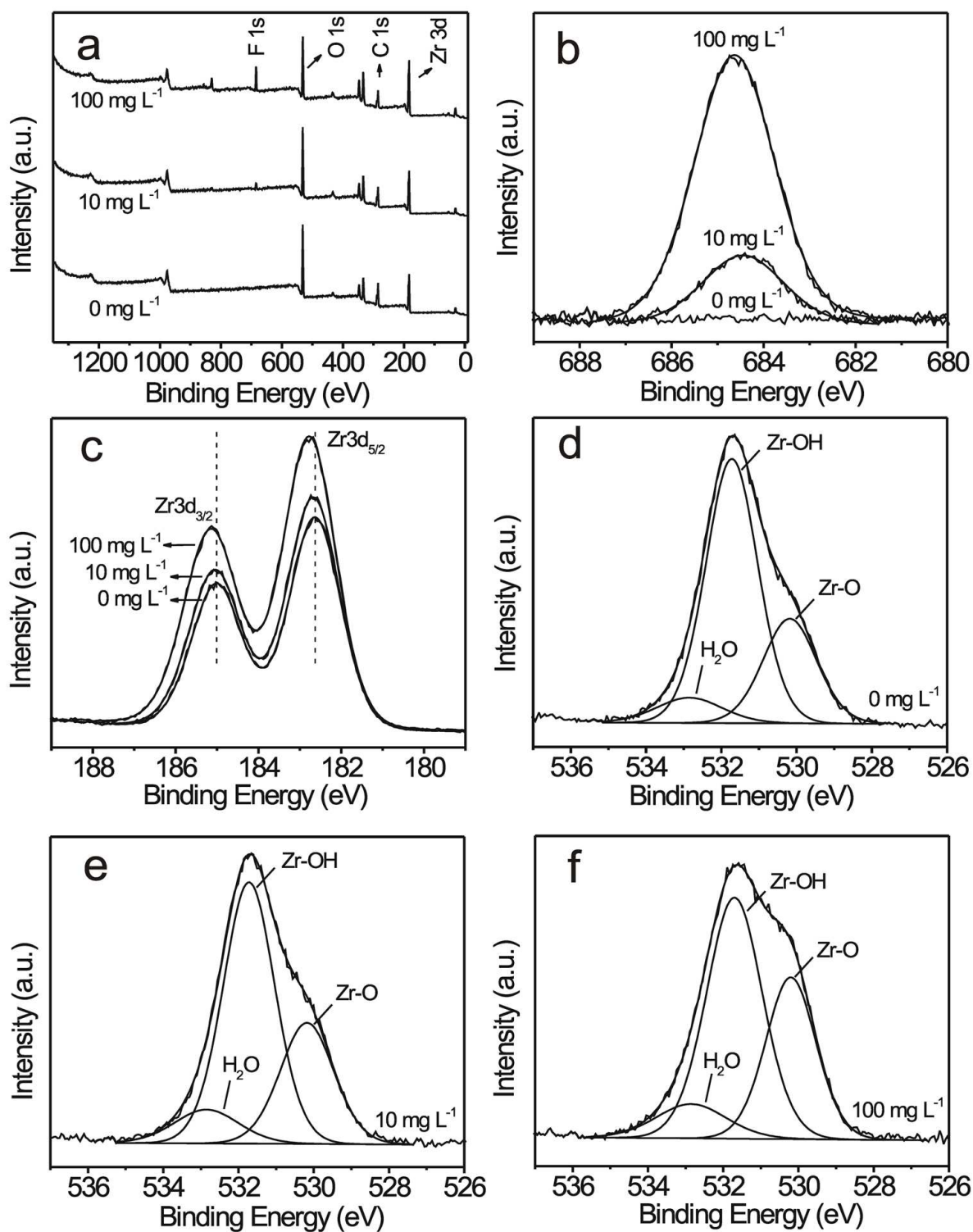


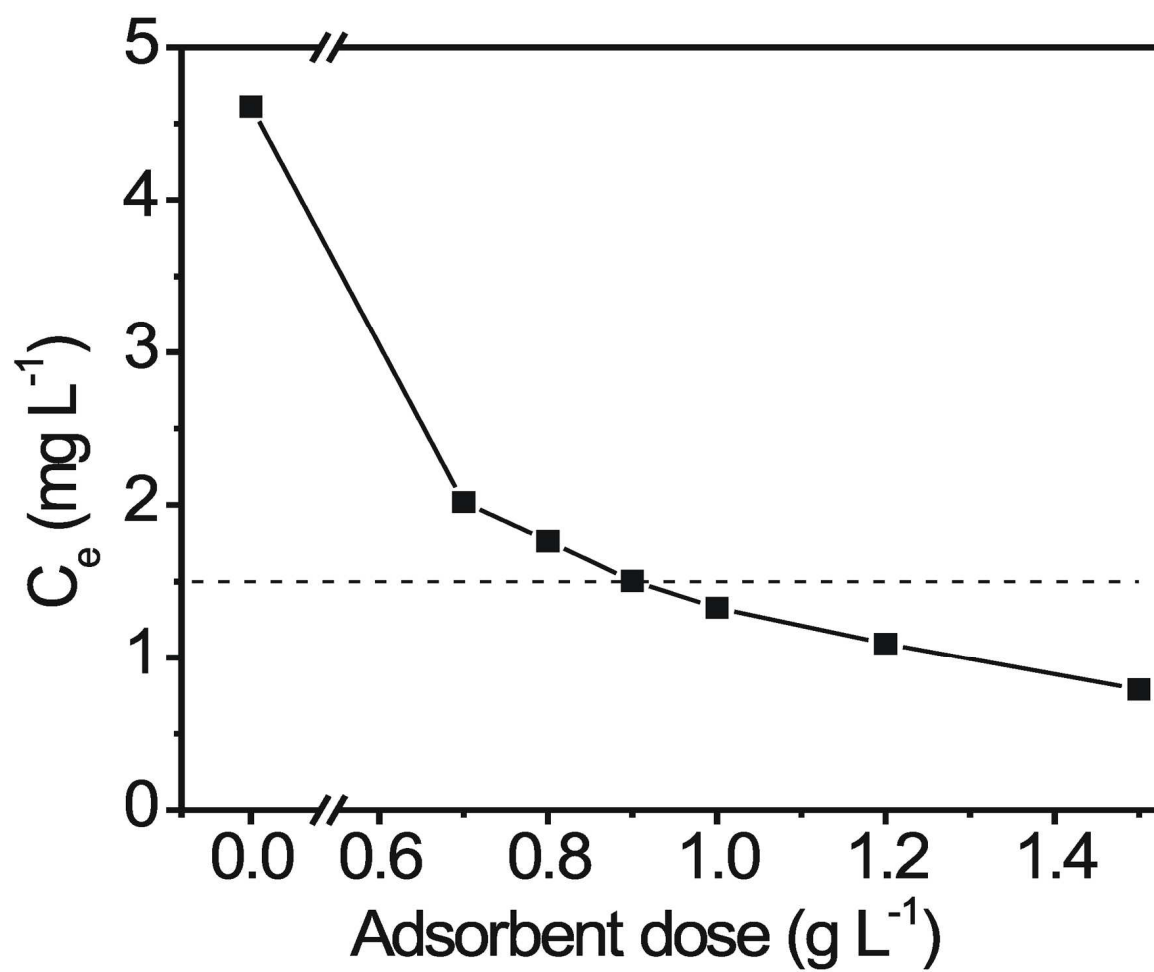












ACCEPTED

Highlights

- Hydrothermally synthesized MOF-801 was used for fluoride removal.
- MOF-801 has high and stable adsorption efficiency at pH 2-10.
- Fluoride adsorption on MOF-801 is not affected by high ion strength.
- Ion exchange of fluoride ions and hydroxyl group in MOF-801 was fully studied.